Application of Conformal Mapping to Rigorous Validation of 2D Coupled EM-CFD Modelling

Konrad Wilczynski[#1], Marzena Olszewska-Placha[$2], Malgorzata Celuch[$3]
[#]Faculty of Physics, Warsaw University of Technology, Poland
[$]QWED Sp. z o.o., Poland
[1]Konrad.Wilczynski@pw.edu.pl, [2]molszewska@qwed.eu, [3]mceluch@qwed.eu

***Abstract*—This paper proposes a quasi-analytical methodology for validating numerical algorithms coupling electromagnetics with heat transfer and fluid flow phenomena. With the increasing interest in Multiphysics modelling in e.g. application of microwave power to biomedical research, it is crucial to prove accuracy of the coupled algorithms as they popularly serve as virtual prototyping tools in the recent research works. For that purpose a conformal mapping technique combined with Fourier series expansion is proposed and compared with coupled FDTD computation for two benchmark models involving microwave heating and fluid flow phenomena.**

***Keywords*—electromagnetic modelling, microwave modelling, microwave heating, fluid flow, analytical solution, conformal mapping, FDTD.**

I. Introduction

Electromagnetic (EM) modelling has a well-established position of a virtual prototyping tool, proven and validated by the decades of research [1-2] and practical, also industrial, applications. Continuously growing interest in application of microwave power to different science domains raised a necessity of analyzing and solving Multiphysics problems. This catalyzed a rapid development of academic [3] and commercial modelling software [4-5] providing a coupling between different physical phenomena. An application of microwave energy to medical treatment [6] and other biomedical research directions caused an increased need for microwave heating analysis further coupled to heat transfer and fluid flow equations [4-5]. As the Multiphysics modelling gains the same role for interdisciplinary research as electromagnetic modelling for microwave engineers, it becomes essential that the numerical analysis delivered by academic and commercial solvers [4-5] is rigorously validated. In papers oriented towards practical applications of coupled EM-CFD solvers [7-8], validation is restricted to *qualitatively* showing that with the changing simulation parameters, the numerical solution changes in accordance with the basic physical intuition. Such an approach, while being a valuable first step, lacks the mathematic rigour of the methodologies well developed for pure EM solvers [1],[9], where the numerical errors are *quantitatively* determined with respect to the physical solutions such as plane waves or eigenmodes in the continuum. To extend the mathematical accuracy studies to coupled EM-CFD solvers, reference coupled scenarios in the continuum need to be defined and solved, which is a challenging task being the purpose of this paper.

The transformation of coordinates techniques are known for decades [10]. Recent research proves them to be increasingly popular and also known as transformation optics in application to metamaterial modelling and FEM-based electromagnetic modelling [11].

In this work, we first propose a canonical coupled EM-CFD benchmark in rectangular coordinates, and then apply the transformation of coordinates to reduce a non-canonical Multiphysics scenario combining EM, heat transfer and fluid flow to a canonical model, which can be solved by Fourier series expansion. Thereby, a reference (quasi)-analytical model for the verification of coupled numerical solution is rigorously derived. Application to 2D coupled EM-CFD problems is provided to corroborate both, a recently implemented FD-TD coupled solver [4], and our benchmarking methodology.

II. Analytical Benchmark - Rectangular Model

In this section we study the time evolution of temperature on a canonical example consisting of rectangular geometry with homogeneous boundary conditions on each wall, either Dirichlet (constant temperature), or Neumann (zero normal derivative of temperature).

A. Governing Equations

The time evolution of the temperature $u = u(x, y, t)$ (°C) in any two-dimensional system with incompressible fluid can be described with the following equations [12-13]:

$$\frac{\partial u}{\partial t} = -\vec{v}(x,y) \cdot \nabla u + k\nabla^2 u + f(x,y) \tag{1}$$

$$f(x,y) = \frac{1}{c_p \rho} \cdot \left(\frac{\sigma |E|^2}{2} + \eta \Phi \right) \tag{2}$$

$$\Phi = \left(\frac{\partial v_y}{\partial x} + \frac{\partial v_x}{\partial y} \right)^2 + 2\left(\frac{\partial v_x}{\partial x} \right)^2 + 2\left(\frac{\partial v_y}{\partial y} \right)^2 \tag{3}$$

where $\vec{v} = [v_x,\ v_y]$ (m/s) stands for fluid velocity distribution, $k = \frac{\kappa}{c_p \rho}$ (m²/s) is the normalized thermal conductivity (where: κ – thermal conductivity (W/(m·°C)), c_p – specific heat capacity under constant pressure (J/(kg·°C)), ρ – density (kg/m³)), σ – electrical conductivity (S/m), $|E|$ – electric field amplitude (V/m), η – dynamic viscosity (Pa·s). Function $f(x,y)$ describes temperature increase resulting from EM heating and internal viscous dissipation, and can have arbitrary spatial distribution, while the thermal conductivity κ has to be uniform over the entire domain. The distribution of fluid

velocity $\vec{v} = [v_x,\ v_y]$ has to be known a-priori and is solved for with the use of equations [12-13]:

$$\rho(\vec{v}\cdot\nabla)\vec{v} - \eta\nabla^2\vec{v} = -\nabla p + \vec{f}, \qquad \nabla\cdot\vec{v} = 0 \tag{4}$$

which correspond to the linear momentum and mass conservation. In (4), p (Pa) stands for the pressure distribution (which is also determined from (4)) and $\vec{f}$ represents external forces per unit volume (N/m^3). For convenience, another equations can be derived from (4), e.g. one can write a Poisson equation to determine the pressure [13]:

$$\nabla^2 p = \nabla\cdot\left(\vec{f} - \rho(\vec{v}\cdot\nabla)\vec{v}\right). \tag{5}$$

B. Geometry and Fluid Velocity Distribution

Fig. 1a presents geometry of the considered rectangular domain $D_{xy} = (0, X)\times(0, Y)$ together with the applied boundary conditions. The temperature assigned at the left side of the rectangle is equal to 0ºC and represents the temperature of the fluid inflowing from left to right. The distribution of fluid velocity, while assuming its zero value at the edges of the channel (for $y = 0$ and $y = g$), has only x component, which is described by the equation:

$$v_x(y) = \frac{\Delta p}{2\eta X}\cdot\left(\left(\frac{g}{2}\right)^2 - \left(y - \frac{g}{2}\right)^2\right), \qquad y\in(0, g) \tag{6}$$

and $v_y \equiv 0$. In (6), Δp (Pa) stands for the pressure difference, which is applied at the left side of the rectangle and forces the fluid flow. The velocity distribution is stationary.

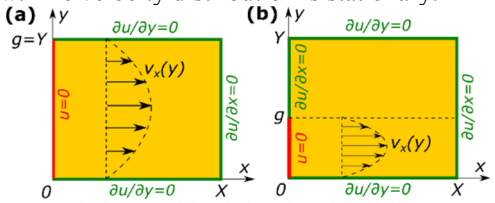

Fig. 1. Schemes of the considered benchmark models: (a) model with homogenous boundary conditions (parameters: X = 100 mm, Y = 10 mm = g), (b) model with inhomogeneous boundary condition on one wall (parameters: X = Y = 50 mm and g = 10 mm).

C. Fourier Series Solution

In order to solve (1) for u, we write the function u as a trigonometrical Fourier series:

$$u(x, y, t) = \sum_{\mu=(n,m)} T_\mu(t)\cdot R_\mu(x, y) \tag{7}$$

$$R_\mu(x, y) = \sin\left(n + \frac{1}{2}\right)\frac{\pi x}{X}\cdot\cos\frac{m\pi y}{Y} \tag{8}$$

where n, m are non-negative integers ($n, m \geq 0$) and we define a numerator $\mu = (n,\ m)$. The functions $R_\mu(x, y)$ form an orthogonal basis and keep the desired boundary conditions. One can now write power dissipation function $f(x, y)$ and components $v_x,\ v_y$ of the fluid velocity as appropriate series of multiplied sine and cosine functions, which, by using trigonometric identities, enables transformation of the entire right-hand side of (1) to a Fourier series over functions $R_\mu(x, y)$. As a result, the following matrix equation is obtained:

$$\frac{d}{dt}\boldsymbol{T} = \widehat{\boldsymbol{C}}\cdot\boldsymbol{T} + \boldsymbol{f} \tag{9}$$

where $\boldsymbol{T}(t) = [T_\mu(t)], \boldsymbol{f} = [f_\mu]$ stand for column vectors of $T_\mu(t)$ and f_μ coefficients, and $\widehat{\boldsymbol{C}} = [c_{\mu\mu'}]$ is a matrix. The coefficients f_μ and $c_{\mu\mu'}$ are defined as:

$$f_\mu = \frac{4\delta_m}{XY}\iint_{D_{xy}} f(x, y)\cdot R_\mu(x, y)dxdy \tag{10}$$

$$c_{\mu\mu'} = \left(n' + \frac{1}{2}\right)\frac{\pi}{X}\cdot V^{(x)}_{\mu\mu'} + \frac{m'\pi}{Y}\cdot V^{(y)}_{\mu\mu'} - K_{\mu\mu'} \tag{11}$$

$$K_{\mu\mu'} = \begin{cases} k\cdot\left(\dfrac{\left(n+\frac{1}{2}\right)^2\pi^2}{X^2} + \dfrac{m^2\pi^2}{Y^2}\right), & \text{if } \mu = \mu' \\ 0, & \text{if } \mu \neq \mu' \end{cases} \tag{12}$$

$$V^{(\xi)}_{\mu\mu'} = v^{(\xi)}_{\substack{n'-n\\ m+m'}} - v^{(\xi)}_{\substack{n+n'+1\\ m+m'}} + v^{(\xi)}_{\substack{n'-n\\ m'-m}} - v^{(\xi)}_{\substack{n+n'+1\\ m'-m}} \tag{13}$$

$$v^{(x)}_{\substack{n''\\ m''}} = \frac{\delta_{m''}}{XY}\iint_{D_{xy}} v_x(x, y)\cdot\sin\frac{n''\pi x}{X}\cdot\cos\frac{m''\pi y}{Y}dxdy \tag{14}$$

$$v^{(y)}_{\substack{n''\\ m''}} = \frac{\delta_{n''}}{XY}\iint_{D_{xy}} v_y(x, y)\cdot\cos\frac{n''\pi x}{X}\cdot\sin\frac{m''\pi y}{Y}dxdy \tag{15}$$

where additionally ξ denotes the coordinate direction: x or y, and δ_n is defined as:

$$\delta_n = \begin{cases}\dfrac{1}{2}, & \text{if } n = 0\\ 1, & \text{if } n \neq 0\end{cases} \tag{16}$$

Note that integers n'', m'' in (14)-(15) can be negative, as contrasted with n, m, n', m' in (7)-(13) which are non-negative. The solution of the matrix equation (9) is found as:

$$\boldsymbol{T}(t) = \exp(\widehat{\boldsymbol{C}}t)\cdot(\boldsymbol{T_0} + \widehat{\boldsymbol{C}}^{-1}\boldsymbol{f}) - \widehat{\boldsymbol{C}}^{-1}\boldsymbol{f} \tag{17}$$

where $\exp(\widehat{\boldsymbol{C}}t)$ is a matrix (defined in terms of Taylor expansion for exponent function), expressed as:

$$\exp(\widehat{\boldsymbol{C}}t) = \widehat{\boldsymbol{N}}\cdot\exp(\widehat{\boldsymbol{D}}t)\cdot\widehat{\boldsymbol{N}}^{-1} \tag{18}$$

where $\widehat{\boldsymbol{N}}$ is a matrix constructed from column eigenvectors $\boldsymbol{c}_n$ of $\widehat{\boldsymbol{C}}$ corresponding to eigenvalues λ_n, and $\exp(\widehat{\boldsymbol{D}}t)$ is a diagonal matrix of expressions $\exp(\lambda_n t)$ in the corresponding order. The column vector $\boldsymbol{T_0} = [T_{\mu 0}]$ is equal to the vector $\boldsymbol{T}(t)$ at $t = 0$, and for any initial temperature distribution $u(x, y, 0)$ the values $T_{\mu 0}$ can be expressed as:

$$T_{\mu 0} = \frac{4\delta_m}{XY}\iint_{D_{xy}} u(x, y, 0)\cdot R_\mu(x, y)dxdy. \tag{19}$$

III. Analytical Benchmark – Arbitrary Geometry

In this section, as a practical illustration, we consider rectangular geometry of Fig. 1b, with an inhomogeneous boundary condition defined on one wall. We study stationary temperature distribution only.

In order to consider and solve this problem, we transform the domain $D_{xy} = (0, X)\times(0, Y)$ to a geometry with homogenous boundary conditions, like described in Section II, defined with new domain, $D_{ab} = (0, A)\times(0, B)$. To achieve this, we implement the conformal mapping from the initial rectangle to the upper half-plane, and back to a rectangle (Fig.2),

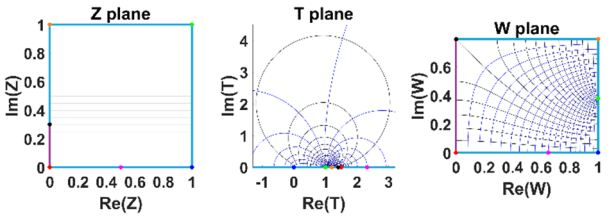

Fig. 2. Conformal transformations applied in this paper, as described in [14]: Z plane (initial rectangle), T plane (upper half-plane), W plane (final rectangle). Purple line indicates Dirichlet boundary condition and blue line – Neumann BC.

following the coplanar waveguide example considered in [14]. The mapping has a form of:

$$w(z) = w(x+iy) = a(x,y) + ib(x,y), \qquad (20)$$

where $a(x,y)$ and $b(x,y)$ are coordinates of the new domain. It can be used to convert (1) in its stationary form to:

$$\left(\tilde{v}_a \frac{\partial}{\partial a} + \tilde{v}_b \frac{\partial}{\partial b} - k \cdot \left(\frac{\partial^2}{\partial a^2} + \frac{\partial^2}{\partial b^2}\right)\right) u = \tilde{f} \qquad (21)$$

where k is constant, $\tilde{f} = f/J$ and:

$$\tilde{v}_a = \frac{1}{J}\left(v_x \frac{\partial a}{\partial x} + v_y \frac{\partial a}{\partial y}\right), \quad \tilde{v}_b = \frac{1}{J}\left(v_x \frac{\partial b}{\partial x} + v_y \frac{\partial b}{\partial y}\right). \qquad (22)$$

Function J in the above equations stands for the jacobian determinant of the transformation:

$$J(x,y) = \begin{vmatrix} \frac{\partial a}{\partial x} & \frac{\partial a}{\partial y} \\ \frac{\partial b}{\partial x} & \frac{\partial b}{\partial y} \end{vmatrix} = \left(\frac{\partial a}{\partial x}\right)^2 + \left(\frac{\partial b}{\partial x}\right)^2 = \left|\frac{dw}{dz}\right|^2, \qquad (23)$$

which is positive ($J > 0$) in the interior of the domain.

In order to solve (21) in the new domain D_{ab}, we assume that the stationary solution in coordinates (a,b) has a form of Fourier series:

$$u(a,b) = \sum_{\mu=(n,m)} u_\mu \cdot \sin\left(n + \frac{1}{2}\right)\frac{\pi a}{A} \cdot \cos\frac{m\pi b}{B} \qquad (24)$$

Coefficients u_μ from the above equation can be collected in a column vector $\boldsymbol{u} = [u_\mu]$, which is equal to:

$$\boldsymbol{u} = -\widehat{\boldsymbol{C}}^{-1}\boldsymbol{f} \qquad (25)$$

where the $\widehat{\boldsymbol{C}}$ matrix and $\boldsymbol{f}$ vector are defined with equations formulated in Section II.C, provided that all x, y, X, Y variables and indexes are replaced with a, b, A, B respectively and the functions v_x, v_y, f in integrals are replaced with $\tilde{v}_a$, $\tilde{v}_b$, $\tilde{f}$. For convenience, double integrals can be calculated in (x,y) coordinates using the following relation:

$$\iint_{D_{ab}} \varphi(a,b) \cdot dadb = \iint_{D_{xy}} \varphi(x,y) \cdot |J(x,y)| \cdot dxdy \qquad (26)$$

which additionally enables to eliminate jacobian determinant $J(x,y)$ from the integrals containing functions $\tilde{v}_a$, $\tilde{v}_b$, $\tilde{f}$.

IV. Simulation Details and Results

A. *Modelling Details*

In order to verify coupled electromagnetic - heat transfer - fluid flow algorithms implemented in commercial modelling tools, we perform the analysis of two benchmark models with the use of both, Fourier series expansion methodology (see Sections II and III) and coupled FD-TD simulations [4]. The benchmark models are defined in a following way:

a) A rectangular model with homogenous boundary conditions (Dirichlet or Neumann) on each wall, as shown in Fig. 1a, for $X = 100$ mm and $Y = 10$ mm $= g$.
b) A rectangular model with inhomogeneous boundary condition on the left-hand wall, as shown in Fig. 1b. The part of rectangle corresponding to $y \in (0, g)$ represents a channel with the fluid. In this case the geometry parameters are: $X = Y = 50$ mm, $g = 10$ mm.

In all the models implemented in the FD-TD microwave simulation we used a parallel-plate systems with the TEM wave propagating perpendicularly to the sheet of dimensions $X \times Y$ and thickness of 2 mm. We used an equidistant mesh with cell size of 1 mm.

The model assumes electrical conductivity of the slab of $\sigma = 0.001$ S/m and the frequency of 2.45 GHz, which corresponds to a penetration depth of 32 cm. This is much greater than the sheet thickness, thereby allows treating the field distribution along slab thickness as homogenous. The amplitude of the incident field was chosen so that the temperature growth rate f_{EM}, related to Joule's heating, was 10°C/s and the heat was being dissipated uniformly over the entire volume. Moreover, with regard to the remaining parameters the following assumptions were made: $\kappa = 1$ W/(m·°C), $c_p = 1$ J/(kg·°C), $\rho = 1000$ kg/m^3, and a high value of viscosity $\eta = 1$ Pa·s was assigned, which enables obtaining stationary fluid flow in less than 0.1 s. The initial temperature was set to 0°C.

B. *Rectangular Model*

The quasi-analytical (Fourier series expansion) and coupled FD-TD results of the temperature profiles, resulting from constant Joule's heating in the benchmark model as in Fig. 1a, are shown in Figs 3-5. The temperature is reported at six time instants, in the long-section $x \in (0, X)$ at $y = Y/2$. The computations were performed for three representative values of average fluid velocities (corresponding to $2/3$ of the maximum value): 0, 1, and 10 cm/s. The quasi-analytical and coupled FD-TD results are in very good agreement. The difference of the maximal reported temperature between the two sets of results, at each time instant and for each fluid velocity, does not exceed 0.2°C.

C. *Arbitrary Geometry*

Figs 6-7 present quasi-analytical (Fourier series expansion) and coupled FD-TD results of the stationary temperature distribution, resulting from constant Joule's heating for the benchmark geometry as in Fig. 1b. The computations were conducted for an average fluid velocities v_{Av} in the fluid channel of 0 and 20 cm/s. The Fourier series expansion approach and coupled FD-TD simulation show consistent temperature distribution in the considered structure. A difference in the maximum temperature value of order of 0.4°C and 1.1°C for v_{Av} equal 0 and 20 cm/s respectively has been observed. Further work is under way to determine, whether the discrepancies originate from the finite FD-TD discretization or finite number of Fourier expansion terms.

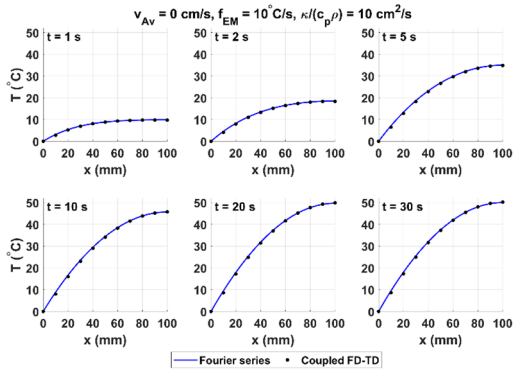

Fig. 3. Temperature profiles (quasi-analytical and coupled FD-TD [4]) in the long-section of the model of Fig. 1a, resulting from constant Joule's heating, for six heating times, when there is no fluid flow.

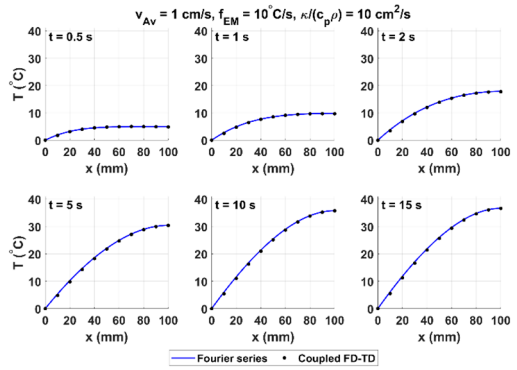

Fig. 4. Temperature profiles (quasi-analytical and coupled FD-TD [4]) in the long-section of the model of Fig. 1a, resulting from constant Joule's heating, for six heating times, for the average fluid velocity of 1 cm/s.

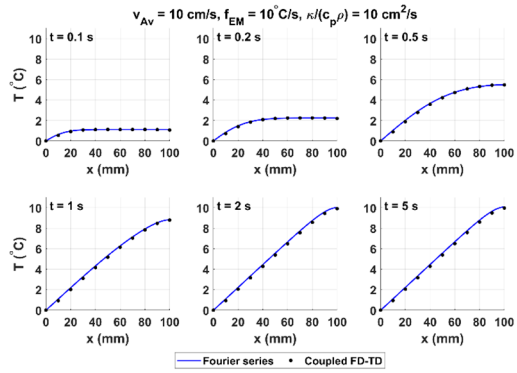

Fig. 5. Temperature profiles (quasi-analytical and coupled FD-TD [4]) in the long-section of the model of Fig. 1a, resulting from constant Joule's heating, for six heating times, for the average fluid velocity of 10 cm/s.

V. Conclusions

This work proposes a methodology for rigorous validation of coupled electromagnetic – heat transfer – fluid flow modelling algorithms implemented in Multiphysics solvers. The methodology is first applied to a canonical benchmark in rectangular coordinates, and it uses coordinates transformation reducing non-canonical problems into canonical ones, which are analogously solved with Fourier series expansion. Two benchmark models are defined and the results of quasi-analytical analysis proposed herein are compared with coupled FD-TD computations. The validation routine proven very good agreement between the obtained results.

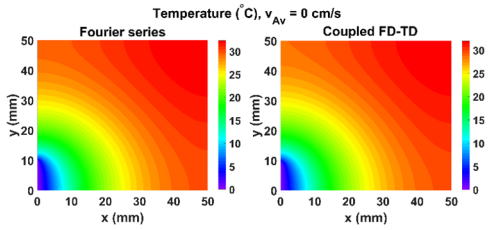

Fig. 6. Maps of the stationary temperature distribution (quasi-analytical and coupled FD-TD [4]) for the model in Fig. 1b for constant and uniform Joule's heating and no fluid flow.

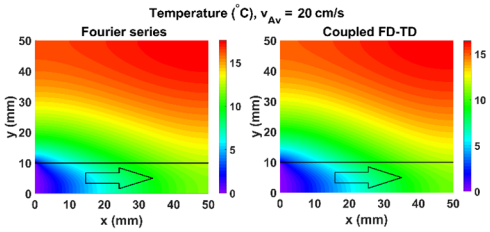

Fig. 7. Maps of the stationary temperature distribution (quasi-analytical and coupled FD-TD [4]) for the model in Fig. 1b for constant and uniform Joule's heating, for the average fluid velocity of 20 cm/s (black line and arrow indicate the fluid channel and direction of the flow).

References

[1] A. Taflove, and S. Hagness, *Computational Electrodynamics - The Finite-Difference Time-Domain Method*, 3rd Edition, Boston-London: Artech House, 2005.

[2] O. C. Zienkiewicz, R. L. Taylor, and J. Z. Zhu, *Finite Element Method – Its Basis & Fundamentals*, 6th Ed., Elsevier Butterworth-Heinemann, 2005.

[3] G. Pelosi, R. Coccioli, and S. Selleri, *Quick Finite Elements for Electromagnetic Waves*, 2nd ed. London: Artech House, 2009.

[4] (2019) The QuickWave EM Software (1997-2019) website. [Online]. Available: http://www.qwed.eu

[5] (2019) COMSOL Multiphysics Software (1986-2019) website. [Online]. Available: https://www.comsol.com

[6] N. Petrovic, I. Tomasic, M. Linden, and P.O. Risman, "Detection of Human Bodypart Abnormalities by Microwaves – A New Approach," *42nd International Convention on Information and Communication Technology, Elecgronica and Microelectronics (MIPRO)*, Opatija, May 2019.

[7] A.A. Mohekar, B. S. Tilley, and V. V. Yakovlev, "A 2D Model of a Triple Layer Electromagnetic Heat Exchanger with Porous Media Flow," *2019 IEEE/MTT-S International Microwave Symposium*, June 2019, pp. 59-62.

[8] S. Patankar, *Numerical heat transfer and fluid flow*. CRC press, 2018.

[9] M.Celuch-Marcysiak and W.K.Gwarek, "On the nature of solutions produced by finite difference schemes in time domain", *Int.J.Numer.Model.*, vol.12, no.1/2, pp.23-40, Jan.-April 1999.

[10] R. E. Collin, Foundations for Microwave Engineering, 2nd ed., McGraw-Hill Inc., 1992.

[11] G. G. Gentili, M. Khosronejad, R. Nesti, G. Pelosi, and S. Selleri, "An efficient 2.5-D finite-element approach based on transformation optics for the analysis of elliptical horns", *IEEE Trans. Antennas Propag.*, Vol. 66, No. 9,Sep. 2018, pp. 4782-4790.

[12] T. L. Bergman, F. P. Incropera, D. P. DeWitt, and A. S. Lavine, *Fundamentals of heat and mass transfer*, John Wiley & Sons, 2011.

[13] J. Cornthwaite, "Pressure Poisson Method for the Incompressible Navier-Stokes Equations Using Galerkin Finite Elements," pp. 1-8, 2013.

[14] T. Sun, H. Morgan, and N.G. Green, "Analytical solutions of ac electrokinetics in interdigitated electrode arrays: Electric field, dielectrophoretic and traveling-wave dielectrophoretic forces," *Physical Review E*, vol. 76, no. 4, Nov. 2007.